

Proposal for an experiment at the FnPB/SNS
pNab: a program of studies of beta decay of polarized free neutrons

R. Alarcon,^a S. Baeßler,^{b,c} L. Barrón Palos,^d L. Broussard,^c J.H. Choi,^e T. Chupp,^f C. Crawford,^g
G. Dodson,^h N. Fomin,ⁱ J. Fry,^j F. Gonzalez,^c J. Hamblen,^k L. Hayen,^l A. Jezghani,^m M. Makela,ⁿ
R. Mammei,^o A. Mendelsohn,^p P. E. Mueller,^c S. Penttilä,^c J. Pioquinto,^b B. Plaster,^g
D. Počanić,^b A. Saunders,^c W. Schreyer,^c A. R. Young.^e

(The pNab Collaboration)

^a Department of Physics, Arizona State University, Tempe, AZ 85287–1504, USA

^b Department of Physics, University of Virginia, Charlottesville, VA 22904–4714, USA

^c Physics Division, Oak Ridge National Laboratory, Oak Ridge, TN 37831, USA

^d Universidad Nacional Autónoma de México, Mexico City, D.F., Mexico

^e Department of Physics, North Carolina State University, Raleigh, NC 27695-8202, USA

^f University of Michigan, Ann Arbor, MI 48109, USA

^g Department of Physics and Astronomy, University of Kentucky, Lexington, KY 40506, USA

^h Massachusetts Institute of Technology, Cambridge, MA 02139, USA

ⁱ Department of Physics and Astronomy, University of Tennessee, Knoxville, TN 37996, USA

^j Department of Physics, Geosciences, and Astronomy, Eastern Kentucky Univ., Richmond, KY 40475, USA

^k Department of Chemistry and Physics, Univ. of Tennessee-Chattanooga, Chattanooga, TN 37403, USA

^l Laboratoire de Physique Corpusculaire, Caen, France

^m Partnership for an Advanced Computing Environment, Georgia Institute of Technology, Atlanta, GA 30332, USA

ⁿ Los Alamos National Laboratory, Los Alamos, NM 87545, USA

^o Department of Physics, University of Winnipeg, Winnipeg, Manitoba R3B2E9, Canada

^p Department of Physics, University of Manitoba, Winnipeg, Manitoba, R3T 2N2, Canada

1 July 2024

Abstract: The Nab and pNab collaborations are undertaking a program of studies of free neutron beta decay with the goal to (1) to determine the ratio of the coupling constants in free neutron beta decay, $\lambda = g_V/g_A$, with unprecedented precision, (2) to contribute to a test of the unitarity of the Cabibbo-Kobayashi-Maskawa matrix, and (3) to search for non-Standard Model forms of weak interaction that manifest themselves as scalar and/or tensor interactions. For this purpose, a large, novel magneto-electrostatic spectrometer, the Nab spectrometer, has been developed, and is being used to determine the correlation coefficients in unpolarized neutron beta decay: a and b . In pNab, the second step, the same spectrometer will be used with a polarized neutron beam to determine two more correlation coefficients, the beta asymmetry A , and the neutrino asymmetry B . The measurements performed in Nab and pNab will provide a robust dataset with unprecedented sensitivity to λ and new physics, and will serve as a needed systematic check to resolve discrepancies in determinations of λ .

1. Scientific motivation

Despite its unparalleled successes, the present Standard Model (SM) of elementary particles and their interactions is known to be incomplete. Additional particles and phenomena must exist. Questions regarding possible extensions of the SM are being simultaneously addressed at the high energy frontier, using particle colliders, and at the precision frontier, using small scale precision experiments. Neutron beta decay contributes to a precision test of the unitarity of the Cabibbo-Kobayashi-Maskawa (CKM) matrix, one of the most sensitive tests of our understanding of the

electroweak interaction of quarks.

The most precise test of the unitarity of the CKM matrix is available for the first row:

$$|V_{ud}|^2 + |V_{us}|^2 + |V_{ub}|^2 = 1 - \Delta \quad (1)$$

To test CKM unitarity, one determines V_{ud} in nuclear or neutron beta decay and V_{us} in certain Kaon decays. The contribution of V_{ub} is too small to register in Eq. (1) at the present level of precision. Current experiments reviewed below indicate $\Delta \sim 10^{-3}$, contrary to the SM expectation of $\Delta = 0$. A failure of the CKM unitarity test indicates new physics, e.g., the effects of additional exchange bosons (e.g., [1, 2]), anomalous couplings (e.g., [3, 4]), or the existence of a fourth quark generation [5, 6]. Refs. [7, 8, 9, 4] use an effective field theory (EFT) approach to show that this test of the CKM unitarity is sensitive to physics with a reach comparable to that of the CERN Large Hadronic Collider, motivating intensive development of new analysis tools which integrate low energy constraints with those from collider measurements.

The most precise determination of V_{ud} is presently obtained from the analysis of superallowed Fermi (SAF) beta decays. The $\mathcal{F}t$ values (the product of “phase space factor”, “(partial) half-life” and “nuclear structure and radiative corrections”) for multiple nuclides undergoing SAF decays are averaged, and are used to determine V_{ud} through

$$|V_{ud}|^2 = \frac{2984.43 \text{ s}}{\mathcal{F}t (1 + \Delta_R^V)} \quad (2)$$

Since 2018, the inner radiative correction Δ_R^V has substantially shifted, and its dominant uncertainty (the contribution of the γW box diagram) has been reduced in Refs. [10, 11, 12, 13, 14]. A preliminary lattice calculation [15] for this contribution in neutron beta decay gets a result similar to the new value for the inner radiative correction.

The analysis of $\mathcal{F}t$ values in SAF decays in Ref. [16] is the one generally adopted. It constitutes a substantial update of previous work: It uses the revised inner radiative correction Δ_R^V , and revised nuclear structure-dependent radiative corrections (commonly called δ_{NS}) that take into account the revised computation of the γW box diagram [17]. The Particle Data Group (PDG) [18] recognizes the new input and gives as the recommended value from SAF decays $V_{ud} = 0.97373(11)_{\text{exp.,nucl.}}(9)_{\text{RC}}(27)_{\text{NS}}$.

There is an opportunity for free neutron beta decay to offer a competitive test of CKM unitarity with Eq. (1), and its potential precision also benefits from the work on the inner radiative correction. The extraction of V_{ud} from neutron and pion beta decay is not affected by nuclear corrections. The triple differential decay rate in neutron beta decay at leading order [19] — assuming T -invariance and no detection of spins of the final state particles — has the form

$$d^3\Gamma \propto \rho(E_e) G_F^2 V_{ud}^2 (1 + 3\lambda^2) \left(1 + a \frac{\vec{p}_e \cdot \vec{p}_\nu}{E_e E_\nu} + b \frac{m_e}{E_e} + \vec{\sigma}_n \cdot \left[A \frac{\vec{p}_e}{E_e} + B \frac{\vec{p}_\nu}{E_\nu} \right] \right) d\Omega_e d\Omega_\nu dE_e \quad (3)$$

The quantity G_F is the Fermi constant, $\rho(E_e)$ is the phase space factor as a function of the (relativistic) electron energy E_e , and σ_n denotes the neutron spin, respectively. Several experiments have measured, or intend to measure, the correlation coefficients a , b , A and B , where $B = B_0 + b_\nu m_e / E_e$. At tree-level in the standard model and upon neglecting terms proportional to the small neutron recoil, the interaction is a pure $V - A$ (vector minus axial vector) for which Fierz interference term b [20] and neutrino Fierz term b_ν vanish. The coefficients a , A , and B_0 depend on $\lambda = g_A / g_V$, the ratio of the Gamow-Teller and Fermi coupling constants, through

$$a = \frac{1 - \lambda^2}{1 + 3\lambda^2}; \quad A = -2 \frac{\lambda^2 + \lambda}{1 + 3\lambda^2}; \quad B = 2 \frac{\lambda^2 - \lambda}{1 + 3\lambda^2} \quad . \quad (4)$$

The parameter λ is most precisely determined by the beta asymmetry A ($dA/d\lambda = -0.37$) and the neutrino electron correlation coefficient a ($da/d\lambda = -0.30$). The neutrino asymmetry B ($dB/d\lambda = -0.08$) is less sensitive to λ . The PDG averages existing experimental results to $\lambda = -1.2754(13)$ with a scale factor of $S = 2.7$. Most of the data used is from measurements of the beta asymmetry A .

The quantity V_{ud} is determined using neutron beta decay data by combining the neutron lifetime τ_n and λ :

$$|V_{ud}|^2 = \frac{5024.7 \text{ s}}{\tau_n (1 + 3\lambda^2) (1 + \Delta_R^V)} \quad (5)$$

The PDG gives the current average lifetime $\tau_n = 878.4(5)$ s, but notes the long-standing disagreement between in-beam ($\tau_{n,\text{beam}}$) and storage-bottle ($\tau_{n,\text{bottle}}$) results.

Figure 1(a) shows a combined analysis of the CKM unitarity test, taken from Ref. [21]. Instead of the usual world average, we have included only the most precise experimental data for λ from a measurement of A in Ref. [22] and τ_n from Ref. [23] from a measurement in a neutron bottle, in evaluating the neutron beta decay limit. The V_{ud} values from SAF and neutrons are consistent. The figure also shows the conflicting limits from kaon decays. The yellow ellipse specifies the 1σ contour of the region with the most likely values for V_{us} and V_{ud} . It misses unitarity by 2.8σ . Inclusion of recent work to obtain V_{us} from tau decays [9] would increase the deviation.

Figure 1(b) allows a closer look at the current neutron beta decay data. The red 1σ bands denote V_{ud} values obtained from neutron lifetimes measured by the bottle method ($\tau_{n,\text{bottle}}$, summarized in [18]) and beam method ($\tau_{n,\text{beam}}$ [24, 25]). The yellow 1σ bands denote values of the ratio λ obtained from the beta asymmetry A (λ_A , compiled in [18]) and from the neutrino-electron correlation a (λ_a , see Refs. [26, 27, 28, 29], with the analysis in Ref. [29] dominating the average). Unlike Fig. 1(b), Fig. 2 shows averages from many neutron beta decay experiments using the method adopted by the PDG [18].

The goal of the Nab experiment [30, 31, 32, 33], currently running at the Fundamental Neutron Physics Beamline (FNPB) of the Spallation Neutron Source (SNS) [34], is to reduce the dominant

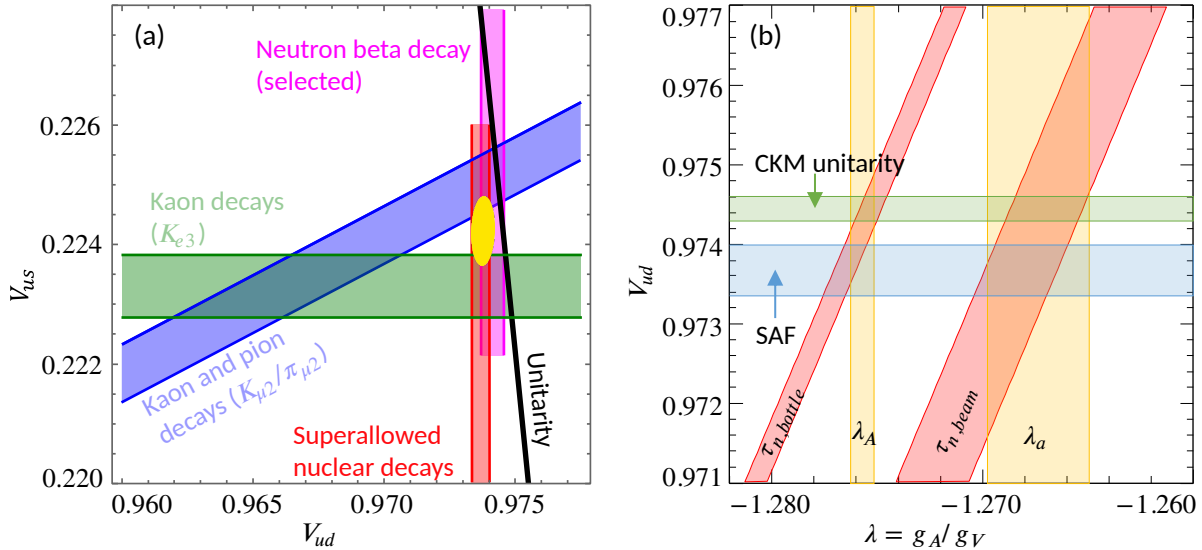


Figure 1: (a) Combined analysis of V_{ud} from selected neutron beta decays and SAF nuclear decays, V_{us}/V_{ud} and V_{us} from kaon and pion decays. If unitarity holds, all 1σ bands have to intersect the black line ($|V_{ud}|^2 + |V_{us}|^2 = 1$) at the same point; here, unitarity is violated by 2.8σ (see [21]). (b) Current 1σ constraints for V_{ud} and λ . Red and yellow neutron beta decay bands are discussed in the text. The blue band denotes the V_{ud} values from SAF and the green band the value from kaons through $|V_{ud}|^2 = 1 - |V_{us}|^2$.

source of uncertainty in the determination of V_{ud} from Eq. (5) by determining the a coefficient and therefore λ with $\Delta\lambda/|\lambda| = 0.04\%$. This measurement may also shed light on the disagreement between λ_A and λ_a . A natural extension of the Nab experiment will make use of the Nab spectrometer, but with a polarized neutron beam, to perform simultaneous measurements of the β -asymmetry A and neutrino asymmetry B involving polarized neutrons. This experiment, called pNab, will require only minor modification of the existing Nab apparatus, since the possibility to have highly polarized neutron beams and precise polarization analysis has been accommodated in the design of Nab. The pNab experiment would provide a new measurement of λ with a goal of $\delta\lambda/|\lambda| = 0.02\%$ and new methods to control sources of systematic uncertainties through coincident detection of electrons and protons and ratios of spin-dependent observables. The Nab and pNab accuracy goals are illustrated with straight red dashed lines in Fig. 2. Note that further progress on the neutron lifetime only makes a substantial impact for the test of the CKM unitarity if it is accompanied with new results with Nab, pNab, or PERC [35, 36]. Besides neutron beta decay, improvements are anticipated in the uncertainty in V_{ud} from the analysis of SAF [37]. There are also planned experiments studying beta decay in mirror nuclei [38, 39] and pions [40] that strive to achieve comparable accuracy in the CKM unitarity test.

Results from pNab will allow a direct comparison with other beta asymmetry measurements entering in λ_A above. There are particular similarities with the UCNAplus project, although pNab

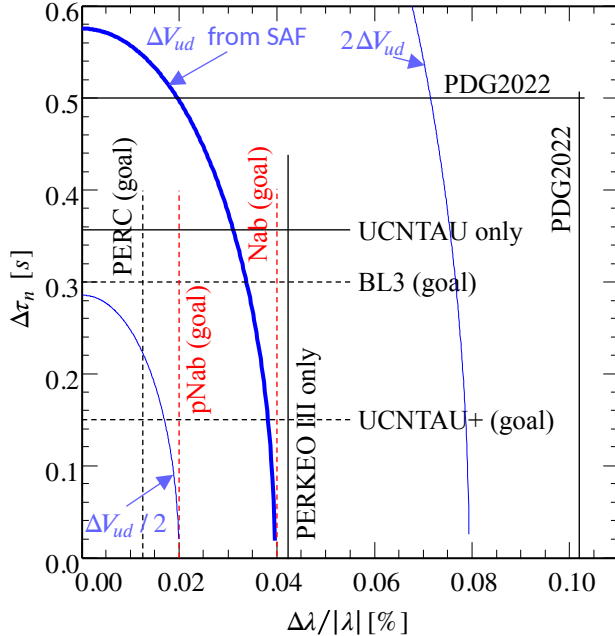


Figure 2: Uncertainty ΔV_{ud} from neutron beta decay (Eq. (5)) as a function of uncertainties in the experimental input. Contours of constant values of ΔV_{ud} are ellipses centered around the origin; shown is the blue thick contour line for ΔV_{ud} from SAF and blue thin contour lines for half and twice that value. The outer vertical and horizontal lines show ΔV_{ud} for neutron beta decay, using averages from [18]; their crossing point far from the origin indicates that PDG’s average is currently not competitive with SAF. The lines denoted “UCNTAU only” and “PERKEO III only” show the selected data set used in Fig. 1(a), which makes neutron beta decay competitive. Dashed straight lines show the impact of experiments under construction.

remains the only coincidence experiment. The outcome of this program is not only a test of the CKM Unitarity that avoids uncertainties due to nuclear corrections. The result can alternatively be interpreted as a test of the CVC hypothesis [41], and as a verification of the new radiative correction calculations.

The ratio λ can be calculated from first principles using Lattice QCD. Recent attempts [42, 43] reach a percent level accuracy. While impressive, this uncertainty is still too large to replace direct measurements. On the other hand, the comparison of calculated and measured λ is a sensitive tool to indicate right-handed currents [44, 38].

Additional tests of the Standard Model can be performed if the electron energy dependences of the correlation coefficients are analyzed; ref. [45] provided a framework in which such an analysis can be performed to verify the weak magnetism term, or to restrict “second class” hadronic matrix elements.

2. Measurement of the beta and the proton asymmetries with the Nab spectrometer

Principles of the Nab spectrometer design and operation are illustrated in Fig. 3. For the current Nab experiment, the polarizer is not present, and the unpolarized cold neutron beam at the FNPB beamline passes through the spectrometer. A tiny fraction of neutrons decay in the fiducial decay volume. Decay protons have to pass through a magnetic filter above the fiducial volume followed by a 5 m flight path. They are detected in the upper Si detector only, which is kept at a high voltage of -30 kV to allow their detection. The Si detectors also accurately measure the energy of the decay electrons with keV-level resolution. Electron energy losses through backscattering of electrons are

largely avoided thanks to the magnetic guide field that connects two Si detectors at both ends of the apparatus. Electrons might bounce, but are ultimately absorbed in the two detectors, whose signals are added. Only events with a total electron energy above a threshold of 100 keV are considered. Energy loss for detector dead-layer and bremsstrahlung have to be taken into account for electron energy extraction. It is addressed using in-situ calibrations using sets of monoenergetic lines from conversion electron sources and additional measurements in test facilities to fully characterize the energy response of the system. Above the magnetic filter, the proton momentum becomes parallel to the magnetic field as the field expands. The measured proton time of flight (TOF) gives an estimate of the proton momentum p_p : for a proton whose momentum is longitudinalized along the magnetic field, we have $p_p \propto 1/t_p$. Finally, the a coefficient and the Fierz term b are extracted from the two-dimensional distribution of events as a function of electron energy and proton TOF.

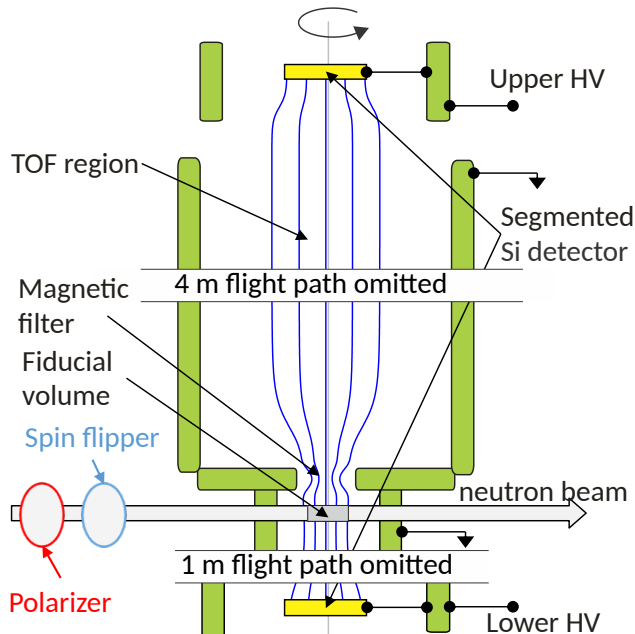


Figure 3: Principles of the design and operation of the pNab spectrometer. Magnetic field lines (shown in blue) and electrodes (light green boxes) possess cylindrical symmetry around the vertical axis. The Nab spectrometer is currently installed at FnPB. With the addition of a neutron beam polarizer (shown as the red oval), the setup becomes the pNab spectrometer.

The asymmetry in the count rate of electrons α_e or protons α_p with respect to the neutron spin can be measured using the Nab spectrometer with minimal modifications; this is the goal of the pNab experiment. Both count rate asymmetries are of the type

$$\text{differential decay rate} \propto (1 + \alpha_{e/p} P_n \cos \theta_0) \quad , \quad (6)$$

where P_n is the degree of polarization of the neutron beam, and θ_0 the initial angle of electron or proton momentum relative to the neutron beam polarization (i.e., the magnetic field) at the moment of the neutron decay. The quantities α_e or α_p are the observables, and may be obtained in dependence of electron energy. To convert α_e into the beta asymmetry A , one uses that $\alpha_e = A \cdot v_e/c$ with electron velocity v_e and speed of light c .

The basic setup is close to what is already installed at FNPB for Nab. The pNab collaboration

will add a neutron polarizer before the Nab spectrometer, and modify the spin flipper to make space for it. Coincidence between electrons and protons from the same neutron decay will be required. For pNab, coincidence is required to suppress background-related uncertainties. The measurement of α_e will use a configuration with an upper electrostatic voltage of 1 kV and a lower voltage of -30 kV, all voltages relative to the fiducial volume, such that all protons are detected in the lower detector. The asymmetry α_p will be measured with the voltage settings exchanged, so that the upper detector serves as the proton detector, like it is currently in the measurement of a with Nab.

Ref. [46] shows how a measurement of the asymmetry in the proton count rate α_p as a function of the electron energy can be transformed into a measurement of the neutrino asymmetry B . Alternatively, one averages over electron energies and obtains $\alpha = C$ (We note that there are different definitions of “proton asymmetry” in the literature; ours follows the most recent measurement [47, 18]). And finally, pNab also allows to analyze the ratio of α_e/α_p in the same instrument with the goal to obtain B/A , as it was done in Ref. [48]. For these measurements, the uncertainty budget has not been completely worked out. The main motivation of all of them is that they allow to determine the neutrino Fierz term b_ν .

2.1. Statistical uncertainty

Table 1 presents the statistical sensitivity of the beta asymmetry A in a Standard Model fit ($b = 0$), and of the Fierz term b (with A as another free parameter). The likely value for the threshold for the electron kinetic energy, $E_{e,\text{kin},\text{min}} = 100$ keV, together with the goal for the statistical uncertainty in $(\Delta A/|A|)_{\text{stat}} = 7 \times 10^{-4}$, translates to a minimum of $N = 5 \times 10^9$ neutron decays in the fiducial volume. The statistical accuracy goal will be reached after about one calendar year, taking into account the published schedule for neutron production at SNS. After only 4 weeks of beam time, pNab would already get to $(\Delta A/|A|)_{\text{stat}} = 0.002$ (this is the uncertainty in the currently most precise result, PERKEO III). These expectations are calculated for a decay rate of 320 s^{-1} and a down time of the experiment (including calibration and other auxiliary measurements) of 25%. This decay rate assumes a transmission of the polarizer of $T_n = 20\%$. The calculations for Table 1 assume perfect neutron beam polarization, which is close to what we want to achieve. In section 2.3 we discuss a beam polarizer that promises to meet these specifications.

Using the same data, we would also be able to obtain $(\Delta b)_{\text{stat}} = 0.007$. We don’t discuss this possibility here, as we hope that by the start of the pNab experiment, we have done a more precise measurement of the Fierz term b with Nab.

2.2. Solid angle acceptance for proton and electron detection

In a symmetric spectrometer such as PERKEO III or UCNA, the measurement precision relies on the fact that the accepted solid angle of each detector is a hemisphere, and the average angle of

Table 1: σ_A , statistical uncertainty in the determination of beta asymmetry A (in a SM fit requiring $b = 0$), and σ_b (obtained in a simultaneous fit with both A and b as fit parameters). Both uncertainties are given as a function of the applied electron energy threshold $E_{e,\text{kin}}$. N is the number of neutron decays in the fiducial volume.

lower $E_{e,\text{kin}}$ cutoff:	none	100 keV	200 keV
σ_A	$4.3/\sqrt{N}$	$4.8/\sqrt{N}$	$7.8/\sqrt{N}$
σ_b	$300/\sqrt{N}$	$350/\sqrt{N}$	$500/\sqrt{N}$

electron (proton) momentum with the neutron spin is given as $\overline{\cos\theta_0} \sim 1/2$ with a correction due to the magnetic mirror effect. The asymmetric spectrometer design of Nab eliminates the uncertainty from an unwanted magnetic mirror effect, and replaces it by the requirement to determine the solid angle of the upper and lower detectors. The cutoff angle for each detector depends on the magnetic field at the position of neutron decay. The measured count rate asymmetries α_e in both detectors can be combined in such a way that the polar angle cutoff for each detector drops out in leading order, or in a different way that allows us to extract the solid angle of the upper detector *in situ* from the beta asymmetries in both detectors. The second possibility is of interest for subsequent use in a measurement of α_p . We have shown in the appendix of Ref. [31] that this works despite unavoidable magnetic field inhomogeneities in the Nab setup. Therefore, no high precision magnetic field measurements are needed, and the systematic uncertainty due to the solid angle is negligible, as is the uncertainty due to the imperfect knowledge of the neutron beam position.

2.3. Neutron beam polarization

A critical point in these measurements will be the precision of the knowledge of the neutron beam polarization. The earlier SNS proposal called for polarizing the neutron beam with a cell containing polarized Helium-3 (see Ref. [49, 50]), and relying on the known time-dependence of the polarization as a tool to analyze it. The advantage is that this provides an in-situ measurement of the degree of polarization. The potential issue is that for a reasonable transmission, the neutron beam polarization is low ($\sim 80\%$) which renders systematic errors hard to detect. The method relies on the assumption that the Helium-3 polarizer is the only device that affects polarization in the beam, an assumption that has not been shown to be true at the required level of precision.

An alternative method, which has been developed, tested, and is being used by scientists at Institut Laue-Langevin (ILL) [51, 52], has the neutron beam polarized with crossed supermirrors to a very high degree ($P_n > 99.7\%$), and analyzed with an opaque polarized Helium-3 spin filter. We argue in this proposal for a new device that builds on the idea of the crossed supermirrors: a modern Solid State Polarizer [53, 54]. Figure 4 shows a sketch of the setup planned for FNPB (the optimization has to be tailored to the beam properties).

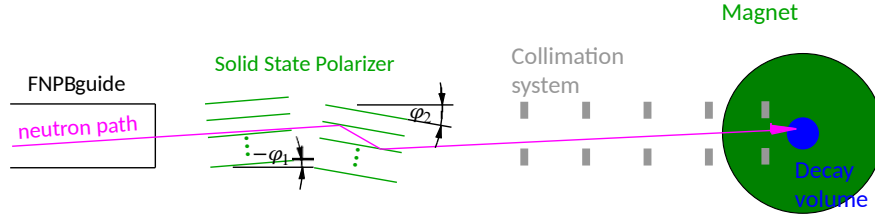


Figure 4: Proposed setup for studies of polarized neutron beta decay with pNab.

The Solid State Polarizer consists of two stacks of $180\ \mu\text{m}$ thin sapphire plates oriented nearly parallel to the neutron beam, coated with modern supermirror and anti-reflective coating on both sides. Most neutrons undergo at least two reflections (and all at least one), guaranteeing a degree of polarization as large as for crossed supermirrors. At the same time, neutron transmission is much higher, as neutrons go on slightly attenuated through a few cm of sapphire substrate, and the only limitation is the imperfect reflectivity of the supermirror-coated surface of the substrate. In contrast, usual supermirror polarizers comprise a stack of thicker and much longer ($30 - 50\ \text{cm}$) glass substrates with gaps in between. The length renders the substrate opaque, and only neutrons that enter through the gaps can be transmitted, with transmission still limited by imperfect reflectivity. Assembly of the Solid State Polarizer will be done in a clean room to avoid dust that could limit the degree of parallelism of the sapphire plates. Simulations for the FNPB predict 99.5% polarization at 40% transmission (just behind the polarizer), which degrades to 99.5% polarization and 20% transmission in the decay volume of the experiment[55, 56]. That simulation takes into account losses in the neutron beam collimation system. Our prediction is similar to the performance to the recently built device at ILL: 99.7% polarization at 33% transmission just behind polarizer [57]. Our optimization is necessarily slightly different since FNPB has a neutron beam with higher divergence. In other words, the Solid State Polarizer combines high polarization and transmission with a quality factor $Q = P_n^2 T_n$ that is superior to a Helium-3 polarizer. Since the through-going beam is not deflected, we have the capability to easily switch back to an unpolarized beam just by removing the polarizer (as it would be for a Helium-3 polarizer, but not a usual supermirror polarizer). The degree of polarization will not show a time dependence unlike it is typical for a Helium-3 polarizer, and the constantly high degree of polarization does not degrade statistical sensitivity of the experiment. In addition, the Solid State Polarizer is now a proven technology.

The systematic uncertainty from imperfect neutron beam polarization ΔP_n will be small due to the fact that the deviation from perfect polarization is small, as demonstrated in all modern beta asymmetry experiments. Correction due to Stern-Gerlach effects have to be applied. We plan to measure the neutron beam polarization with opaque Helium-3 cells. We are estimating the uncertainty to be $\Delta P_n \leq 5 \times 10^{-4}$, corresponding to a relative uncertainty in the beta asymmetry

of $\Delta A/A \leq 5 \times 10^{-4}$. We want to be conservative in our promises: This is only slightly better than what had been achieved with a worse-performing polarizer in PERKEO III [22], and substantially less precise than what the experienced ILL group plans to do with the same technique for PERC.

2.4. Electron energy calibration

The pNab experiment plans to use the same detector system as the one used in Nab. The simulated electron energy response of the Nab detector system is shown in Fig. 5(a). Its width is substantially smaller than it was for plastic scintillator detectors used in previous experiments. A set of radioactive calibration sources will be used to determine the detector response function, and to establish the linearity of the relationship between deposited energy and ADC channel. The sources are backed by thin, e.g., $10 \mu\text{g}/\text{cm}^2$, carbon foils, and are movable within the fiducial volume so as to reach every point in the detector. Six candidates for such calibration sources have been used in Ref. [58]. Possible deviations from perfect linearity of the relationship between pulse height and deposited energy are shown in Fig. 5(b). Table 2 shows the requirements on the detector response to achieve desired measurement uncertainties. The requirements for the measurement of the beta asymmetry A are much less stringent than for measurements of a and b coefficients with Nab”. Detector design and modelling are described in Refs. [59, 60, 61, 62].

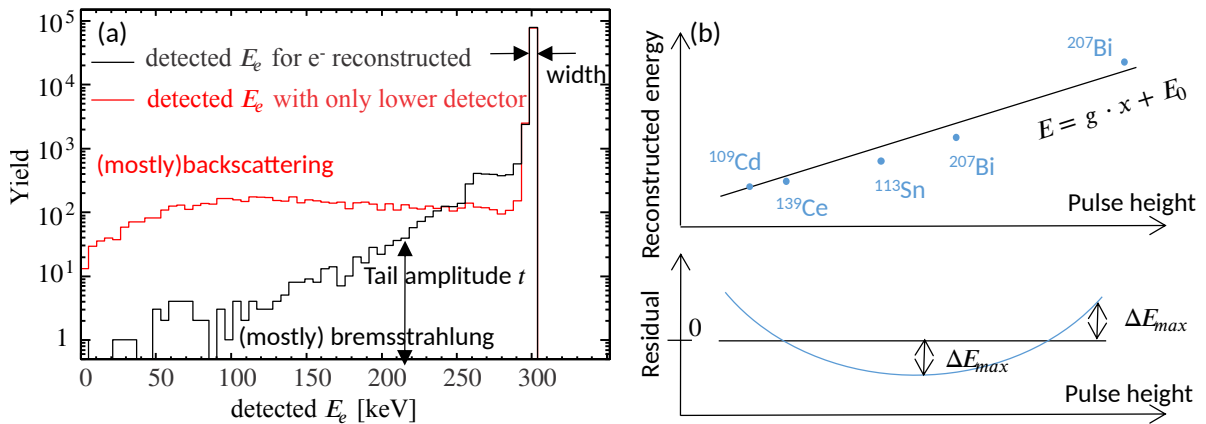


Figure 5: (a) Simulated detector electron energy response for electrons incoming with $E_e = 300 \text{ keV}$. The red curve is for a single detector, and shows a large tail due to electron backscattering. The black curve is for both detectors. Backscattering is suppressed, and the remaining tail is mostly due to Bremsstrahlung. (b) Relationship between energy deposited in a detector and the average pulse height of the output signal. These synthetic data exaggerate possible types of nonlinearity.

Fig. 6 shows a preliminary spectrum of the electrons from Sn-113 source taken during Nab commissioning in summer 2023. The raw energy spectrum is the energy deposition in a single detector. The spectrum of reconstructed events gives the reconstructed energy derived from all hits in both detectors of each event. The flat tail due to backscattering is strongly reduced, as predicted in the simulation in Fig. 5(a). There is a remaining exponential tail that may be due

Table 2: Requirements on our understanding of the detector response for the planned measurements with Nab and pNab. The meaning of the parameters are explained in Fig. 5.

Specification for	$\Delta a = 3 \times 10^{-5}$ (Nab)	$\Delta b = 10^{-3}$ (Nab)	$\Delta A = 3 \times 10^{-5}$ (pNab)
Gain factor ($\Delta g/g$)	fit parameter	fit parameter	0.0018
Offset E_0	0.3 keV	0.06 keV	0.2 keV
Nonlinearity ($ \Delta E_{\max} $)	1.5 keV	0.06 keV	0.3 keV
Tail to peak ratio (Δt)	0.01%	0.2%	2.4%

to energy deposition in inoperable pixels which were present in that beamtime, or due to the high threshold used for the detection of additional hits. The Nab collaboration is currently working on the elimination of both problems.

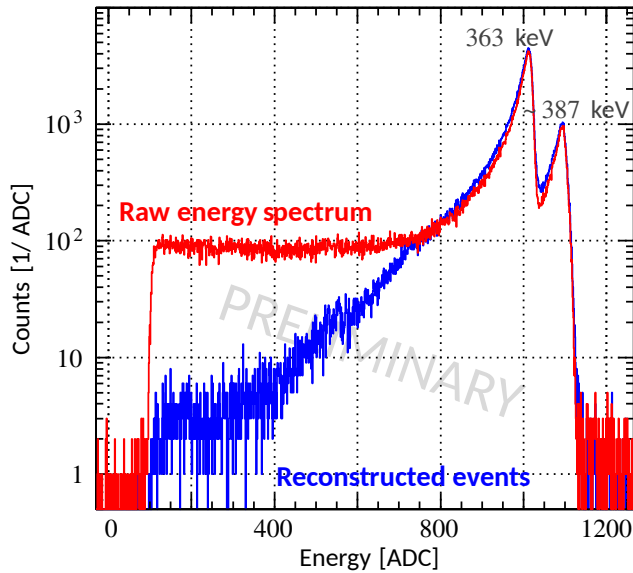


Figure 6: Preliminary spectrum of electrons from a Sn-113 source. The two main decay electron energies are marked. The red line shows the energy spectrum obtained from a single detector. The blue line shows the spectrum of reconstructed energies that take into account energy depositions in both detectors.

2.5. Electric field homogeneity

Protons from decays in a shallow electrostatic potential minimum with a momentum close to parallel to the magnetic field are trapped, which affects the solid angle of detector acceptance. A measurement of α_p in a symmetric spectrometer is very difficult: Unwanted electrostatic potential variations need to be reduced to well below 1 mV, which is hard to achieve and even harder to verify. The asymmetric Nab spectrometer is much better suited for a proton asymmetry measurement: Only protons whose momentum points mostly upwards can pass the filter in Nab. Protons which are trapped in the decay volume would not pass the filter even in the absence of an unwanted trap, and therefore make no difference for α_p . In Nab, the leading contribution to the list of uncertainties from unwanted electrostatic potential variations is a potential difference between the filter region and the fiducial volume. A filter–fiducial volume potential difference as large as 100 mV changes

the proton asymmetry by less than 0.01%, and can be neglected. The main electrode system for Nab suppresses potential differences far below this requirement [63].

The beta asymmetry is much less sensitive to trapping, as electron energies are much higher.

3. Budget and schedule

The pNab experiment needs a modest amount of funds in addition to what has been spent or committed already for the Nab experiment. A budget is shown in Table 3. This is in addition to the operating expenses of 250 k\$ per year that is needed for upkeep of the Nab experiment at the beamline.

Table 3: Budget estimate for pNab

Item	Budget [k\$]	Contingency [k\$]
Solid State Polarizer	150	350 ^a
Additional Si Detectors	100	25
Changes to beamline	150	75
Total	400	450

^a The polarizer budget item reflects material costs only, and assumes that we can complete the assembly and characterization with our students and in collaboration with scientists of the host institution (the ILL). The large contingency is for the case that the Solid State Polarizer has to be purchased.

Furthermore, pNab will require the continuation of personnel commitment from ORNL similar to that required for Nab. In particular, pNab will need substantial support from the beamline staff to prepare for and carry out the Instrument Readiness Review, and to a lesser degree for interfacing with SNS and ORNL support staff during operations.

The changeover from Nab data-taking to the start of the pNab experiment is expected to take about 3 months. The main activity is to install the polarizer and a shortened spin flipper, and determine the degree of polarization with sufficient precision. Since pNab can make use of all other systems of the Nab experiment, no further commissioning is needed if pNab is directly following the Nab experiment. After only 2 months of data taking, the result allows to test CKM Unitarity with the same precision as SAF. Within one year of data taking, the statistical goal of pNab is reached. Note that this time estimates should be increased by 50% if a reasonable amount of time contingency is to be included.

A decision on pNab has to be made well before Nab data taking is ending: Funds need to be available early enough to start contracting and fabrication of the the longest lead-time item, which is the Solid State Polarizer. Fabrication of this device takes at least one year.

The estimates assume that Nab has indeed finished data-taking before pNab starts. pNab will

rely on the detector characterization that has to be performed for Nab. In this document, the pNab collaboration proposes a followup experiment after Nab has finished its data-taking, not a replacement or a reason for a premature termination of Nab.

4. Summary

The pNab experiment co-proposing research groups commit to forming a collaboration with the goal of reaching the ultimate sensitivity to new physics at the Fundamental Neutron Physics Beamline at the Spallation Neutron Source with pNab. The pNab experiment is to be staged at the FnPB immediately following the completion of measurements with unpolarized neutrons in the Nab experiment, and it will re-use most of the existing Nab apparatus. The most significant hardware addition will be a novel, custom design high efficiency supermirror polarizer that the pNab collaboration proposes to fabricate and use. The measurement program with pNab is expected to take only about an additional year plus schedule contingency, as pNab will make use of the characterization program of the elements of the Nab spectrometer that will have to be done for Nab anyway. Carrying out pNab will require only modest additional resources.

The pNab experiment goal is a measurement of the neutron beta asymmetry to substantially better than $\Delta A/A = 10^{-3}$, as indicated in Fig. 2. The main systematic uncertainties in this measurement are related to the determination of the neutron beam polarization and to the detector, and pNab will have an important synergy with the Nab experiment in that the detector characterizations made for Nab are more than sufficient for pNab. Together, Nab and pNab measurements will provide a unique study of the CKM matrix unitarity, with very different systematics compared to other existing or planned measurements. CKM unitarity appears to be violated by about 3σ since new, more precise calculations of the inner radiative correction became available, making the proposed pNab extension to Nab well motivated.

Acknowledgements

If approved, the research proposed here would use resources at the Spallation Neutron Source, a U.S. Department of Energy (DOE), Office of Science User Facility operated by the Oak Ridge National Laboratory. This proposal would not be possible without the prior investment in the Nab superconducting spectrometer, custom detectors, and other components of the Nab experiment. We acknowledge the support for the Nab experiment from DOE, the National Science Foundation, the University of Virginia, Arizona State University, the Natural Sciences and Engineering Research Council of Canada, and Triangle University Nuclear Laboratory.

References

1. W. Marciano, A. Sirlin, Phys. Rev. D **35**, 1672 (1987)
2. A. Kurylov, M. Ramsey-Musolf, Phys. Rev. Lett. **88**, 071804 (2000)
3. S. Alioli et al., J. High En. Phys. **05**, 086 (2017)
4. V. Cirigliano et al., arXiv: 2311.00021
5. W. Marciano, A. Sirlin, Phys. Rev. Lett. **56**, 22 (1986)
6. P. Langacker, D. London, Phys. Rev. D **38**, 886 (1988)
7. V. Cirigliano et al., Nucl. Phys. B **830**, 95 (2010)
8. M. Gonzáles-Alonso et al., Prog. Nucl. Part. Phys. **104**, 165 (2019)
9. V. Cirigliano et al., J. High En. Phys. **04**, 152 (2022)
10. C.-Y. Seng et al., Phys. Rev. Lett. **121**, 241804 (2018)
11. C.-Y. Seng et al., Phys. Rev. D **100**, 013001 (2019)
12. A. Czarnecki et al., Phys. Rev. D **100**, 073008 (2019)
13. L. Hayen et al., Phys. Rev. D **103**, 113001 (2021)
14. K. Shiells et al., Phys. Rev. D **104**, 033003 (2021)
15. P.-X. Ma et al., arXiv: 2308.16755
16. J.C. Hardy, I.S. Towner, Phys. Rev. C **102**, 045501 (2020)
17. M. Gorchtein, Phys. Rev. Lett. **123**, 042503 (2019)
18. R.L. Workman et al. (Particle Data Group), Prog. Theor. Exp. Phys. **2022**, 083C01 (2022), and 2023 update
19. J.D. Jackson et al., Phys. Rev. **106**, 517 (1957)
20. M. Fierz, Z. f. Phys. **104**, 553 (1937)
21. V. Cirigliano et al., Phys. Lett. B **838**, 137748 (2023)
22. B. Märkisch et al., Phys. Rev. Lett. **122**, 242501 (2019)
23. F.M. Gonzalez et al., Phys. Rev. Lett. **127**, 162501 (2021)
24. J. Byrne et al., Europhys. Lett. **33**, 187 (1996)
25. A.T. Yue et al., Phys. Rev. Lett. **111**, 222501 (2013)
26. Ch. Stratowa et al., Phys. Rev. D **18**, 3970 (1978)
27. J. Byrne et al., J. Phys. G **28**, 3125 (2002)
28. F.E. Wietfeldt et al., arXiv:2306.15042

29. M. Beck et al., Phys. Rev. Lett. **132**, 102501 (2024)
30. D. Počanić et al., Nucl. Inst. Meth. A **611**, 211 (2009)
31. S. Baeßler et al., J. Phys. G **41**, 114003 (2014)
32. J. Fry et al., Eur. Phys. J. Web Conf. **219**, 04002 (2019)
33. S. Baeßler et al., submitted to Eur. Phys. J. Web Conf.
34. N. Fomin et al., Nucl. Instr. Meth. A **773**, 45 (2015)
35. D. Dubbers et al., Nucl. Instr. Meth. A **596**, 238 (2008)
36. X. Wang et al., Europ. Phys. J. Web Conf. **219**, 04007 (2019)
37. C.-Y. Seng, M. Gorchtein, Phys. Lett. B **838**, 137654 (2023)
38. L. Hayen, A. Young et al., arXiv: 2009.11364
39. L. Hayen, arXiv: 2403.08485
40. W. Altmannshofer et al., arXiv: 2203.01981
41. D. Dubbers, M.G. Schmidt, Rev. Mod. Phys. **83**, 1111 (2011)
42. R. Gupta et al., Phys. Rev. D **98**, 034503 (2018)
43. C.C. Chang et al., Nature **558**, 91 (2018)
44. V. Cirigliano et al., Prog. Part. Nucl. Phys. **71**, 93 (2013)
45. S. Gardner, B. Plaster, Phys. Rev. C **87**, 065504 (2013)
46. F. Glück et al., Nucl. Phys. A **593**, 125 (1995)
47. M. Schumann et al., Phys. Rev. Lett. **100**, 151801 (2008)
48. Yu.A. Mostovoi et al., Phys. At. Nucl. **64**, 1955 (2001)
49. S.I. Penttila, J.D. Bowman, J. Res. Natl. Inst. Stand. Technol. **110**, 309 (2005)
50. R. Alarcon et al., abBA experiment proposal, available at http://nab.phys.virginia.edu/ABBA_proposal_2007.pdf, (2007)
51. M. Kreuz et al., Nucl. Inst. Meth. A **547**, 583 (2005)
52. Ch. Klauser et al., Phys. Proc. **42**, 99 (2013)
53. A.K. Petoukhov et al., Nucl. Inst. Meth. A **838**, 33 (2016)
54. A.K. Petoukhov et al., Rev. Sci. Instr. **90**, 085112 (2019)
55. L. Shen, University of Virginia, internal report (2021)
56. J. Pioquinto, University of Virginia, internal report (2024)

57. A.K. Petoukhov et al., Rev. Sci. Instrum. **94**, 023304 (2023)
58. H. Abele et al., Phys. Rev. Lett. **88**, 211801 (2002)
59. A. Salas Bacci et al., Nucl. Instr. Meth. A **735**, 408 (2014)
60. L. Broussard et al., Nucl. Instr. Meth. A **849**, 83 (2017)
61. L. Broussard et al., Hyp. Int. **240**, 1 (2019)
62. L. Hayen et al., Phys. Rev. C **107**, 065503 (2023)
63. H. Li, Ph.D. thesis, University of Virginia, 2021, arXiv: 2402.13559